

Carbon nanotubes as a 1D template for the synthesis of air sensitive materials: About the confinement effect

**J.P. Tessonier, G. Winé, C. Estournès, C. Leuvrey, M.J. Ledoux
and C. Pham-Huu**

Laboratoire des Matériaux, Surfaces et Procédés pour la Catalyse (UMR 7515 du CNRS), ECPM-ULP, 25 rue Becquerel, F-67087 Strasbourg Cedex 2, France
Institut de Physique et Chimie des Matériaux de Strasbourg (UMR 7504 du CNRS), ULP, 23 rue du Loess, F-67037 Strasbourg Cedex 2, France

Abstract

Cobalt ferrite and cobalt iron nanowires with an average diameter of 50 nm and lengths up to several micrometers were synthesized inside multi-walled carbon nanotubes (MWNTs) under mild reaction conditions, i.e. 100 °C and atmospheric pressure, using an aqueous nitrate precursor salt filling the tubes. The concept of a confinement effect inside carbon nanotubes has been advanced to explain the formation of CoFe_2O_4 under such mild reaction conditions. The formation of caps near the tube tips at the beginning of the nitrate decomposition meant that each nanotube was considered as a closed nanoreactor, in which the reaction conditions could be very different to the macroscopic conditions outside the tube. The subsequent reduction of the CoFe_2O_4 allowed to obtain CoFe nanowires cast in the carbon nanotubes. These nanowires exhibit a high resistance towards oxidation, whereas bulk CoFe is known to undergo oxidation at room temperature and atmospheric pressure. This phenomenon was attributed to oxygen diffusion problems due to the confinement effect of the carbon nanotubes.

Keywords: Nanowires; Multi-walled carbon nanotubes; Confinement effect; Nanoreactor

1. Introduction
 2. Experimental
 3. Results and discussion
 4. Conclusion
- References

1. Introduction

Carbon nanostructures, nanotubes and nanofibers, the smallest organized form of carbon, have received an increasing scientific interest, from a fundamental point of view as well as for their physical properties, and for several of their potential applications ranging from living matter structure manipulation to nanometer-sized computer circuits [1], [2], [3] and [4], all this since their discovery at the beginning of the last decade by Iijima as a by-product in the arc-discharge synthesis [5]. The inner diameter of the multi-walled carbon nanotubes (MWNTs) can vary from few nanometers to several dozens depending on the nature of the synthesis method, i.e. arc-

discharge, laser ablation or chemical vapor deposition [4], [6] and [7]. Both the single-walled carbon nanotubes (SWNTs) and the MWNTs exhibit an extremely high aspect ratio (length-to-diameter ratio) ranging from 30 to more than many thousands [8]. It was expected that the tubular morphology and the high aspect ratio of MWNTs could induce a confinement effect on the gas or the liquids trapped inside the tube leading to completely different physical behavior when compared to conventional bulk material. Several reports recently dealt with the behavior of water trapped inside MWNTs [9], [10], [11], [12], [13], [14] and [15]. The most detailed study was reported by Gogotsi and co-workers [14] and [15]. They reported that water and gas trapped inside the tubes rapidly reached the supercritical state under heating because of the confinement effect induced by the surrounding wall. Nanotubes can also be used to protect sensitive products against aggressive media. Dravid [16] has reported that nickel particles introduced inside the nanotubes were not damaged even after storage for several months in an aqua regia solution.

In addition, introduction of foreign elements inside the carbon tubules can give rise to peculiar effects either on the properties of the filling element or of the filled carbon nanotube. Ajayan et al. [17] used the surface-tension effect to fill carbon nanotubes with vanadium oxide, which can be used in the catalytic oxidation process, at relatively high filling temperature, i.e. 1023 K. However, it should be stressed that the filling selectivity remained relatively low, filled and externally coated carbon nanotubes both being present in the final sample. Recently, Xu et al. [18] have reported the filling of single-walled carbon nanotubes with lanthanide halide by heating an intimate mixture of carbon nanotubes and halide above the melting point of this halide. These encapsulated material can be subsequently used in several potential domains including magnetism and catalysis fields.

Metallic single elements or alloys of iron and cobalt made up of nanoclusters are extremely useful owing to their peculiar properties compared to the bulk metal or oxide counterparts either for magnetic or catalysis applications [19], [20], [21] and [22]. However, the use of metallic nanocluster materials was hampered by the high oxidation behavior of these materials in the presence of air.

The aim of the present work is to report the use of multi-walled carbon nanotubes as a template with a confinement effect for the synthesis of CoFe_2O_4 nanowires under mild conditions and their subsequent transformation into CoFe alloy nanowires. Thanks to the high aspect ratio of the MWNT template, the metallic alloy exhibits a relatively high resistance towards oxidation in air, allowing an easy handling and storage. This work is also motivated by the possible application of these metallic alloy nanowires directly as catalyst.

2. Experimental

Purified open MWNTs with mean outer and inner diameters of 100 and 60 nm, respectively, and lengths up to several micrometers (Applied Surface Science, OH, USA) were used as template. The CoFe_2O_4 nanowires were synthesized as follows: the iron and cobalt precursors salts (14.47 g $\text{Fe}(\text{NO}_3)_3 \cdot 9\text{H}_2\text{O}$ and 4.94 g of $\text{Co}(\text{NO}_3)_2 \cdot 6\text{H}_2\text{O}$) were first dissolved in a volume of water and ethanol (60 ml, 90% distilled water and 10% ethanol) corresponding to the inner volume of the carbon tubule, previously determined by analysis of a statistical sample of microscopy images. Carbon nanotubes (10 g) were then added without further purification. The metal loading was set to be ca. 30%. The filling of the carbon nanotubes was possible thanks to capillary forces, the surface tension of the solution ($<72 \text{ mN m}^{-1}$) being lower than the critical surface tension reported in the literature for the carbon nanotubes (190 mN m^{-1}). The filled material was then dried in air in an oven (Nabertherm model L3/11/P320) at 100°C for 2 h in order to remove the excess of water.

The calcination of the sample at 450 and 600°C was performed in a Thermolyne 21100 furnace

equipped with a tubular quartz reactor, respectively, under flowing air and flowing helium ($50 \text{ cm}^3 \text{ min}^{-1}$, heating rate $10 \text{ }^\circ\text{C min}^{-1}$), during 2 h. The reduction of the CoFe_2O_4 into CoFe was performed in the same furnace under flowing hydrogen ($50 \text{ cm}^3 \text{ min}^{-1}$) at $400 \text{ }^\circ\text{C}$ during 2 h (heating rate $10 \text{ }^\circ\text{C min}^{-1}$).

The crystallinity of the sample was characterized by powder X-ray diffraction technique (XRD) using a non-monochromatic $\text{Co K}\alpha$ source. The location of the sample with respect to the carbon nanotubes and the microstructure was followed by means of transmission electron microscopy (TEM) with a Topcon 002B microscope working at 200 kV accelerating voltage with a point-to-point resolution of 0.17 nm.

3. Results and discussion

The drying of the filled material in air at $100 \text{ }^\circ\text{C}$ for 2 h induced the formation of a needle-like CoFe_2O_4 with a short-range crystallinity (Fig. 1A). Increasing the heating temperature from 100 to $450 \text{ }^\circ\text{C}$ led to the modification of the nanowire microstructure, i.e. the hair-like CoFe_2O_4 was transformed into a more crystallized material (Fig. 1B). The nanowire microstructure again drastically changed when the heating temperature was increased up to $600 \text{ }^\circ\text{C}$ (Fig. 1C).

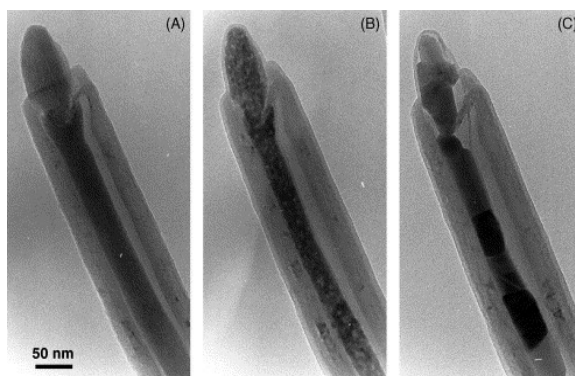


Fig. 1. In situ TEM micrographs recorded as a function of the heating temperature of the CoFe_2O_4 cast inside MWNT: (A) $100 \text{ }^\circ\text{C}$; (B) $450 \text{ }^\circ\text{C}$; and (C) $600 \text{ }^\circ\text{C}$.

The CoFe_2O_4 particles of the sample after heat treatment at $600 \text{ }^\circ\text{C}$ became big enough to be detected by the XRD technique. The mean particle size deduced from the Scherrer formula was ca. 35 nm, which was still relatively small owing to the reduction temperature. The details of the synthesis procedure have already been published elsewhere [23].

The formation of the CoFe_2O_4 hair-like structure after heat treatment at $100 \text{ }^\circ\text{C}$ of the impregnated sample was attributed to the confinement effect of the surrounding MWNT. After 10 min of heating at $100 \text{ }^\circ\text{C}$, part of the water was vaporized leading to the formation of a semi-permeable amorphous CoFe_2O_4 solid cap at the tube tip, which in turn modifies the pressure inside the tube (Fig. 2A). The non-decomposed nitrate precursor remains trapped inside the tubes and continues to decompose under a higher local pressure leading, after 30 min at $100 \text{ }^\circ\text{C}$, to the formation of a low ordered CoFe_2O_4 nanowire with a hair-like microstructure (Fig. 2B).

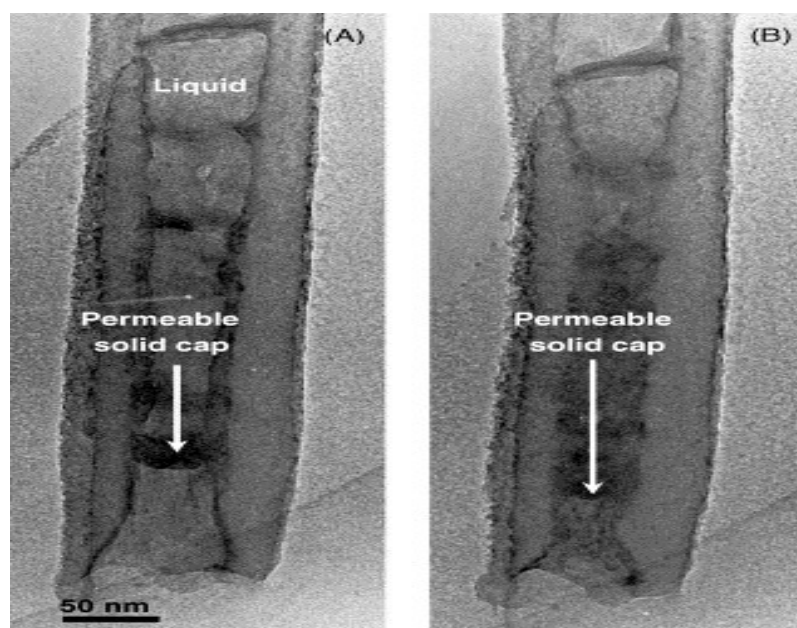


Fig. 2. In situ TEM images of the permeable solid cap, i.e. amorphous CoFe_2O_4 phase, formation from the nitrate solution under electron beam heating during 10 min (A) and 30 min (B). The length of the permeable solid cap formed as a function of heating time was schematized by an arrow with increasing length.

Such a pressure increase would be similar to that involved in hydrothermal synthesis of zeolites and probably enhances the rate of CoFe_2O_4 formation from its mother nitrate solution under mild synthesis conditions, i.e. $100\text{ }^\circ\text{C}$. Mössbauer spectrum of ^{57}Fe nuclei was recorded at 4.2 K and confirmed the nature of the phase present in the MWNT tubule after the 30 min heating at $100\text{ }^\circ\text{C}$ (Fig. 3).

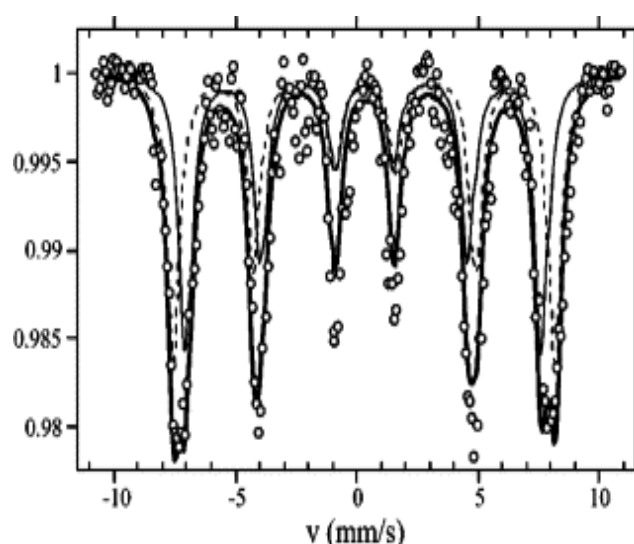


Fig. 3. Mössbauer spectrum recorded at 4.2 K on the nanowires filling the sample of carbon nanotubes after air treatment at $100\text{ }^\circ\text{C}$. Experimental points (\circ), iron ions in octahedral (...) and tetrahedral (—) sites and the resulting fit (\square).

The formation of solid caps at the tube tips led to consider the inside of each nanotube like a closed nanoreactor. The non-decomposed nitrate precursor remaining trapped and blocked by the caps inside the tubes could see local synthesis conditions, different from those outside the tubes.

The local pressure inside the tubes, i.e. a nanoscopic pressure, could be greater than the macroscopic pressure which remained unchanged outside the tubes. The strength of MWNTs could allow this pressure increase inside the nanotubes without being destroyed. It has recently been reported by Gogotsi et al. [15] that fluids pressurized around 30 MPa at room temperature could be trapped inside MWNTs with an outer diameter of 100 nm, without having destroyed the tubes. This confinement effect, in terms of increase in the reactant partial pressure inside the tubes, has already been advanced to explain kinetically the gain in catalytic performance when using silicon carbide nanotubes as catalyst support instead of the analogue grain-based material for supporting the phase active for the hydrogen sulfide selective oxidation into elemental sulfur [24].

The TEM image of the CoFe alloy cast inside carbon nanotube after reduction of the parent CoFe_2O_4 at 400 °C is presented in Fig. 4. The reduction temperature was deliberately kept lower than 600 °C in order to avoid any gasification of the surrounding carbon nanotubes by reaction with hydrogen, which could lead to the formation of methane and thus carburization of the CoFe alloy. Separate experiments carried out (not reported) have shown that the carburization starts at temperature of about 680 °C. The relatively low-temperature reduction allowed the complete retention of the 1D morphology of the material. A high-magnification TEM image (not shown) revealed that the alloy nanowire was made up of small particles with an average diameter of ca. 30–40 nm. Higher magnification in order to obtain further insight into the microstructure of the material was not possible due to the thickness of the material.

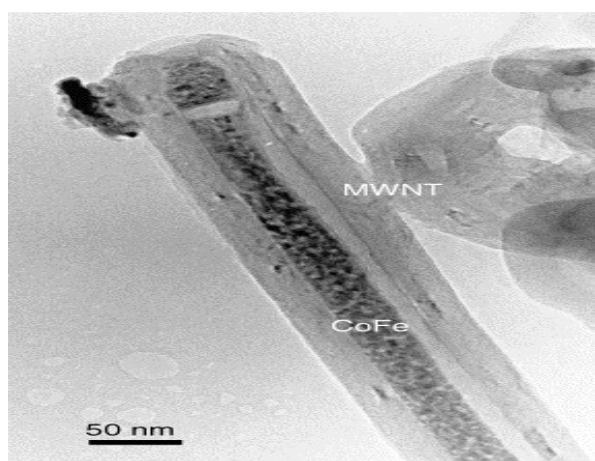


Fig. 4. The CoFe_2O_4 sample after heat treatment at 600 °C and after reduction in flowing hydrogen at 400 °C. The contrast generated inside the reduced sample was attributed to the density change when going from CoFe_2O_4 to CoFe, which lead to the formation of voids inside the nanowire structure.

The XRD pattern (Fig. 5) confirmed the complete reduction of the parent CoFe_2O_4 into its corresponding metallic alloy while the nanowire morphology was completely retained during the reduction process. The average metallic particle size deduced from the X-ray line broadening was around 36 nm, which was in good agreement with that observed by TEM. It is worth noting that the XRD pattern indicates the complete absence of any other phases, i.e. single oxide or carbide, in the samples reduced at temperature up to 400 °C which was not the case for high temperature encapsulation where a significant amount of carbide was observed due to the solid–solid reaction between the encapsulated material and the carbon material or through a gas-phase reaction during the preparation step [25], [26] and [27].

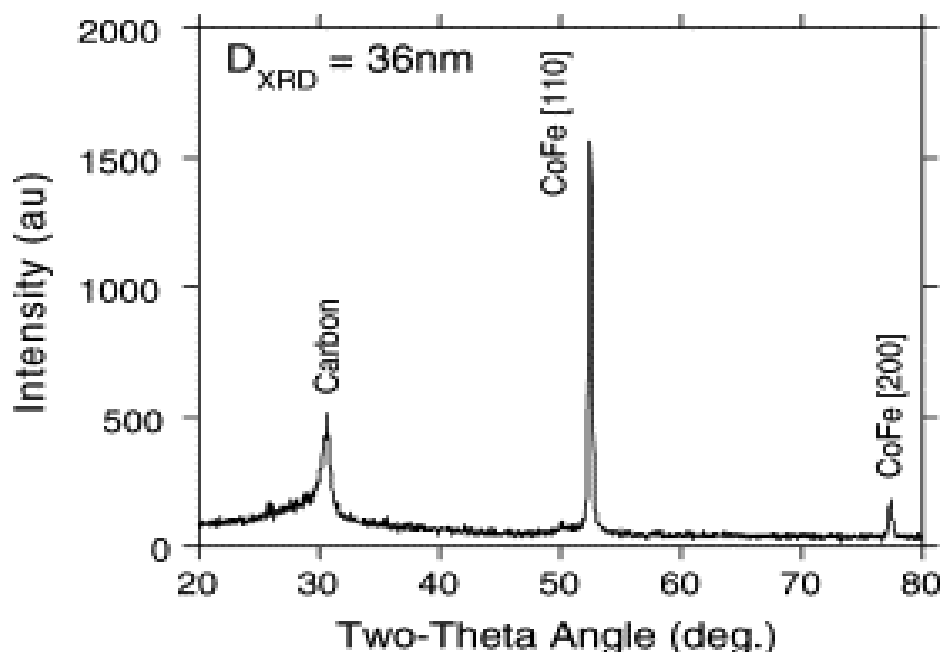


Fig. 5. XRD pattern of the CoFe alloy reduced in flowing hydrogen at 400 °C for 2 h showing the high selectivity of the reduction process.

The oxidative resistance of the alloy was evaluated using an in situ high-temperature X-ray technique. The sample was heated in air from room temperature to 500 °C and a XRD pattern was recorded every 50 °C in order to check the phase transformation during heating. The results obtained are presented in Fig. 6. It is worth noting that the same CoFe alloy without carbon nanotubes surrounding was completely oxidized back to its corresponding parent oxide after exposure to air at room temperature. The observed results were in good agreement with those reported in the literature about the extremely high air sensitivity of the metallic alloy nanoclusters.

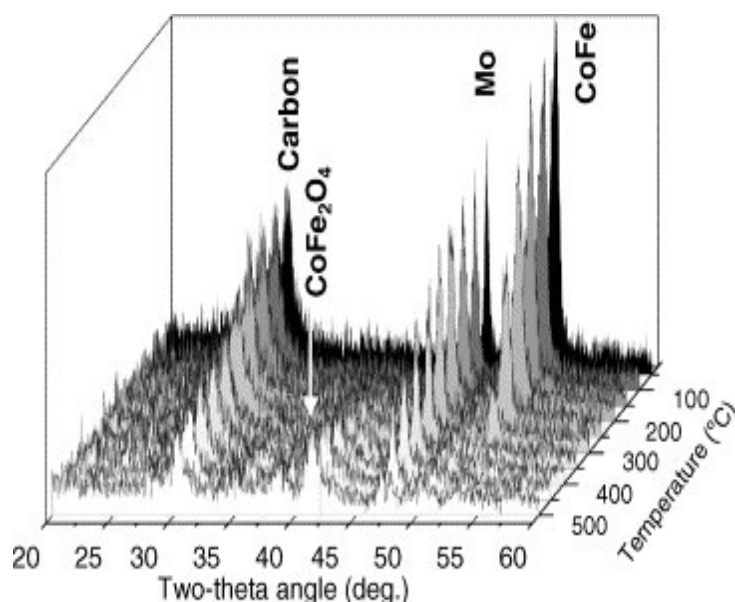


Fig. 6. In situ high-temperature XRD patterns of the CoFe alloy during heating in air at different temperatures. The diffraction line corresponding to the Mo element was originated from the sample holder. It is worth noting that the same sample without carbon nanotube steadily combusted back to the CoFe₂O₄ phase after air exposure at room temperature.

On the other hand, the carbon cast nanoclusters metallic alloy showed a relatively high resistance towards air oxidation as no trace of CoFe_2O_4 was observed even after heating up to 200 °C. At temperatures higher than 200 °C, an oxidation process started to occur and a diffraction line corresponding to the CoFe_2O_4 phase was observed in the XRD pattern. At 350 °C, the complete oxidation occurred and the XRD pattern only showed a diffraction line corresponding to the CoFe_2O_4 phase. The results observed clearly indicate that most ferromagnetic nanoclusters casted inside the multi-walled carbon nanotubes were well protected by the surrounding graphene planes. The high oxidative resistance of the CoFe cast samples could also be attributed to the high aspect ratio of the MWNT, which hindered oxygen diffusion inside the tube under atmospheric pressure and thus prevented the complete oxidation of the cast CoFe nanowire encountered with the naked sample.

4. Conclusion

In summary, 1D ferromagnetic nanoclusters can be efficiently prepared using multi-walled carbon nanotubes as a controlling size template by a simple and reproducible method working at relatively low temperature. The as-synthesized sample exhibits a relatively high oxidative resistance as no oxidic peaks were detected even after heating in air up to 200 °C. Apparently, a combination of the high aspect ratio and the small free space between the surrounding carbon nanotube wall and the ferromagnetic alloy hindered oxygen diffusion inside the tube, thus avoiding the excessive oxidation of the sample as observed for its naked metallic counterpart. This example shows the exciting possibility of using such carbon nanomaterials as nanoscale reactors and opens new perspectives for preparing highly anisotropic nanomaterials for catalytic applications. Work is ongoing to check these 1D CoFe metallic alloy as catalyst and will be presented soon.

References

M.S. Dresselhaus, G. Dresselhaus and P.C. Eklund, Editors, *Science of Fullerenes and Carbon Nanotubes*, Academic Press, London (1996).

In: T.W. Ebbesen, Editor, *Carbon Nanotubes: Preparation and Properties*, CRC Press, Boca Raton (1997).

H. Dai, *Acc. Chem. Res.* **35** (2002), p. 1045.

P.M. Ajayan, *Chem. Rev.* **99** (1999), p. 1787.

J.M. Bonard, L. Forro, D. Ugarte, W.A. de Herr and A. Châtelain, *ECC Res.* **1** (1998), p. 9 and references therein.

K.T. Lau and D. Hui, *Compos.: Part B Eng.* **33** (2002), p. 263 and references therein.

E.T. Thostenson, Z. Ren and T.W. Chou, *Compos. Sci. Technol.* **61** (2001), p. 1899.

S. Iijima, *Nature (London)* **354** (1991), p. 56.

C. Laurent, E. Flahaut, A. Peigney and A. Rousset, *New J. Chem.* (1998), p. 1229 and references therein.

Y.H. Hu and E. Ruckenstein, *J. Catal.* **134** (1999), p. 298.

M.A. Ermakova, D.Y. Ermakov, G.G. Kuvshinov and L.M. Plyasova, *J. Catal.* **187** (1999), p. 77.

V. Lordi and N. Yao, *J. Mater. Res.* **15** (2000), p. 2770.

K. Koga, G.T. Gao, H. Tanaka and X.C. Zeng, *Nature* **412** (2001), p. 802.

- M.S.P. Sansom and P.C. Biggin, *Nature* **414** (2001), p. 156.
- M.C. Gordillo and J. Marti, *Chem. Phys. Lett.* **341** (2001), p. 250.
- R.E. Tuzun, D.W. Noid, B.G. Sumpter and R.C. Merkle, *Nanotechnology* **7** (1996), p. 241.
- (a) J. Libera and Y. Gogotsi, *Carbon* **39** (2001), p. 1307.
(b) Y. Gogotsi, N. Naguib and J.A. Libera, *Chem. Phys. Lett.* **365** (2002), p. 354.
- Y. Gogotsi, J.A. Libera, A.G. Yazicioglu and C.M. Megaridis In: A.M. Rao, Editor, *Nanotubes and Related Materials, Materials Research Society Symposium Proceedings, vol. 633* Pittsburgh, Pennsylvania (2001), pp. A7.4.1–A7.4.6.
- V.P. Dravid, *Nature* **374** (1995), p. 602.
- P.M. Ajayan, O. Stephan, Ph. Redlich and C. Colliex, *Nature* **375** (1995), p. 564.
- C. Xu, J. Sloan, G. Brown, S. Bailey, V.C. Williams, S. Friedrichs, K.S. Coleman, E. Flahaut, J.L. Hutchison, R.E. Dunin-Borkowski and M.L.H. Green, *Chem. Commun.* (2000), p. 2427.
- X. Li and S. Takahashi, *J. Magn. Magn. Mater.* **214** (2000), p. 195.
- C. Pham-Huu, B. Madani, P. Leroi, S. Savin-Poncet, J.L. Bousquet, PCT/FR04/03380 (2003).
- G.H. Lee, S.H. Huh, J.W. Jeong and H.C. Ri, *J. Magn. Magn. Mater.* **246** (2002), p. 404.
- A.E. Berkowitz and R.M. White, *Mater. Sci. Eng. B* **3** (1989), p. 413.
- C. Pham-Huu, N. Keller, C. Estournès, G. Ehret and M.J. Ledoux, *Chem. Commun.* (2002), p. 1882.
- J.M. Nhut, R. Vieira, L. Pesant, J.P. Tessonnier, N. Keller, G. Ehret, C. Pham-Huu and M.J. Ledoux, *Catal. Today* **76** (2002), p. 11.
- Z.H. Wang, C.J. Choi, B.K. Kim, J.C. Kim and Z.D. Zhang, *Carbon* **41** (2003), p. 1751.
- X.L. Dong, Z.D. Zhang, Y.C. Chuang and S.R. Jin, *Phys. Rev. B* **60** (1999), p. 3017.
- X.C. Sun, A. Gutierrez, M.J. Yacaman, X.L. Dong and S. Jin, *Mater. Sci. Eng. A* **286** (2000), p. 157.

Corresponding author. Tel.: +33 3 90 24 26 75; fax: +33 3 90 24 26 74.

Member of ELCASS (European Laboratory for Catalysis and Surface Science).

Original text : Elsevier.com